**Proceedings of the ASME 2011 International Design Engineering Technical Conferences &
Computers and Information in Engineering Conference
IDETC/CIE 2011
August 28-31, 2011, Washington, DC, USA**

DETC2011-47184

OPTIMAL SYNTHESIS OF A NEW SPHERICAL PARALLEL MECHANISM FOR APPLICATION TO TELE-ECHOGRAPHY CHAIN

M. A. LARIBI
Institut PPRIME - DGMSC
CNRS-Université de Poitiers–ENSMA
UPR 3346, France
med.amine.laribi@univ-poitiers.fr

T. ESSOMBA
PRES Loire Valley University,
Université d'Orléans, Laboratoire Prisme
France
terence.essomba@etu.univ-orleans.fr

S. ZEGHLOUL
Institut PPRIME - DGMSC
CNRS-Université de Poitiers–ENSMA
UPR 3346, France
said.zeghloul@univ-poitiers.fr

G. POISSON
PRES Loire Valley University,
Université d'Orléans, Laboratoire Prisme
France
gerard.poisson@bourges.univ-orleans.fr

ABSTRACT

This paper considers the practice of a tele-echography through a new slave holder robot for a remote echographic diagnostic application. This robot is integrated in a master-slave system called 'Robotic Platform for an Interactive Tele-echographic System' (PROSIT ANR French national project).

The proposed approach is based on motion capture of an expert's gestures during the echography examination. The medical gestures were analyzed in terms of positions and velocities; the result has been used in the definition of the kinematics specifications of the proposed manipulator.

The effective workspace size of a standard echography act, done by the medical expert, is determined through an experimental study. The evaluation of the workspace is based on the use of the Vicon Nexus motion capture system. The spherical parallel mechanism (SPM) has been selected because of its characteristics meeting the constraint requirements. In addition this architecture offers an excellent stiffness, high precision and is light weight.

The design problem of a new parallel probe-holder robot according to the identified experimental workspace for the tele-echography system is presented.

In this work, in order to increase the workspace volume of the manipulator, a minimal set of geometrical parameters of spherical parallel manipulators are optimized to find the maximum workspace. Seven independent design parameters have been identified.

The optimal synthesis of spherical parallel manipulators is performed using a real-coded genetic algorithm (GA) based method. An optimal study of the orientation workspace is also presented.

INTRODUCTION

Among many types of medical equipment, ultrasound diagnostic systems are widely used because of their convenience and innocuity. Performing ultrasound examination involves good hand-eye coordination and the ability to integrate the acquired information over time and space. Tele-echography is, therefore, an interesting alternative to conventional care. Development of a high-performance remote diagnostic system, which enables an expert operator at the hospital to examine a patient located far from the expert, in an emergency vehicle, or in a remote clinic may have a very significant clinical added value.

In this domain, existing works can be structured in two subdomains: works exclusively related to the telemedicine aspect, mainly image transmission and manipulation (see, for instance, TeleinVivo [1]), and works integrating robotic assistance to the expert. A subclass of systems allows automating an echographic examination using a robot (see [2]–[3]). A second category of robot-based systems enables the remote examination of patients by a distant expert with [4], [5] or without [6], [7], [8] force feedback. This is especially the case for patients living in isolated areas with reduced or substandard medical facilities.

In this work, we propose to study medical gestures in the aim of proposing a new architecture adapted for tele-echography system. An optimal synthesis of a new spherical parallel mechanism is performed. Robot workspace definition

in the literature can be cast into two classes: (i) finding the workspace of a given mechanism; and (ii) producing a mechanism with a desired workspace. In this paper, we focus on the second approach. For a general spatial robot, the workspace is made of a positional workspace and an orientation workspace. The positional workspace is the volume swept by a point of the end effector during its motion. The orientation workspace is, however, more difficult to represent and it is defined as the set of all possible orientations of the end effector. These problems have attracted substantial attention among researchers. Affi et al. [9] carried out the dimensional synthesis and optimization of the workspace of a 3-transalational-dof in-parallel manipulator. Kosinska et al. [11] presented an algorithm for the synthesis of a DELTA parallel manipulator in order to have its workspace contain a set of specified points. Laribi et al. [10] presented a genetic algorithm based optimal dimensional synthesis method of the DELTA parallel robot for a described workspace. All these works were concerned with the positional workspace. The problem of the orientation workspace is, however, more complex and only a few works investigating this problem can be found in the literature ([12], [13], [14], [15]). In general, the orientation workspace of a spherical parallel manipulator (SPM) is rather small due to the characteristics of its closed kinematic chain.

The main focus of this paper is the slave robot. The SPM is designed to have a maximum size of its orientation workspace. A genetic algorithm (GA) is used to solve the optimization problem, because of its robustness and easy of use.

The paper is organized as follows: Section II is devoted to the general presentation of the Robotic Platform for an Interactive Tele-echographic System, as well as the presentation of the motion capture and analysis of an expert's gestures. The experimental results of the motion capture of the position and orientation of the probe are presented. Section III defines the slave robot and focuses on its mechanical architecture. The kinematic analysis of the SPM and the determination of its workspace are provided. In Section IV, we carry out the formulation of the optimization problem using the genetic algorithm technique. Section V is dedicated to conclusions and perspectives.

THE OVERVIEW OF THE TELE-ECHOGRAPHY SYSTEM

Description

The master-slave system called 'Robotic Platform for an Interactive Tele-echographic System' (PROSIT ANR French national project) allows the medical expert in echography to operate a slave robot which holds an ultrasound probe on a patient located in the distant site. The expert can control the robot by moving a virtual probe in a manual, natural, and unconstrained way and the system safely reproduces these motions.

The slave robot holds and moves a real echographic probe as specified by the distant expert. The obtained ultrasound images are continuously sent from the slave site to the expert that has to perform the examination and provide a diagnosis.

This work focuses on the slave robot. We analyzed echographic examinations in order to design the tele-echography operating protocol and specify the slave robot motion. Thus, to determine the motion of the remote echography system, the executed motions of a real echography probe were analyzed while an expert was examining a patient under a conventional procedure.

MOTION CAPTURE AND ANALYSIS

The motion capture method is based on the experience of the biomechanics community [9] especially for the choice of marker sets location and segment reference definitions. Computer graphics [10] focus on the use of motion capture and synthesis movement to generate three-dimensional realistic movements for virtual models.

The collected kinematics data is based on the use of the Vicon Nexus motion capture system. The observed volume is about 1m long, 1m high, and 0.5m wide.

Fourteen reflexive markers (Figure 1) are placed on the subject (expert hand + probe). The markers placed on the expert's hand are not used here for the motion analysis, only the ones on the probe are treated.

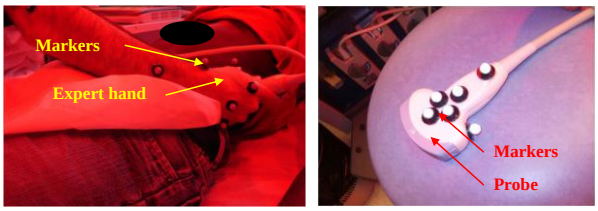

Figure 1: Expert hand and probe markers set.

Using Nexus software, we identify the three coordinates of each marker at each moment, in the reference coordinates system, when it is visible.

Using the data obtained, we can reconstruct the entire probe movement of a probe. For these calculations, we distinguish the reference coordinates system, R_0, and the local coordinates system of the probe, R_P.

To extract any segment (Part is considered as undeformable) movements in the reference coordinate system R_0, three markers are needed to build the segment coordinate system.

For motion analysis, only three markers are needed, but we added a fourth one for the event that one of them is hided during the movement. This has significantly increased our computing capability.

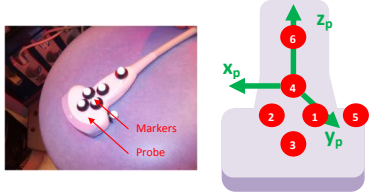

Figure 2 : Layout and numbering of markers on the probe.

The rotation matrix of the segment is built from the definition of this coordinate system as described below

$$Rot(x_{(S/R_0)} \quad y_{(S/R_0)} \quad z_{(S/R_0)})$$

The coordinates system of the probe is built at every moment of recording. A general rotation matrix can have the form as follows:

$$R = \begin{bmatrix} x_X & y_X & z_X \\ x_Y & y_Y & z_Y \\ x_Z & y_Z & z_Z \end{bmatrix} \begin{matrix} \leftarrow \vec{x}_0 \\ \leftarrow \vec{y}_0 \\ \leftarrow \vec{z}_0 \end{matrix}$$

with $\vec{x}_P$, $\vec{y}_P$, $\vec{z}_P$ as the column vectors.

We calculate the position and orientation of the probe coordinate system. It is possible to express the transformation from first to second frame using three successive rotations.

The Euler angles: precession ψ, nutation θ and own rotation φ are used to characterize the probe orientation and thus the conical workspace, (Figure 3).

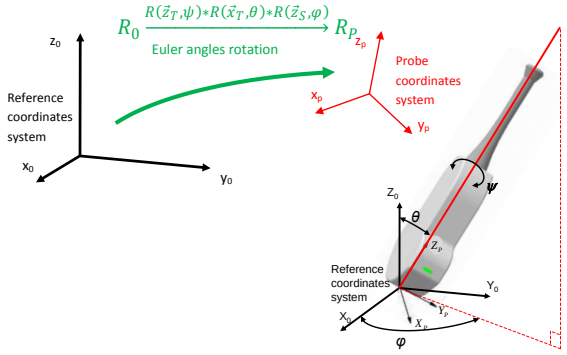

Figure 3 : Reference and probe coordinates systems**.**

Euler angles are identified from the transformation matrix. This matrix can be thought of as a sequence of three rotations, one about each principle axis. Since matrix multiplication does not commute, the order of the axes which one rotates about will affect the result. For this analysis, we will rotate first about the Z-axis, then the X-axis, and finally the Z-axis. Such a sequence of rotations can be represented as the matrix product,

$$Re = R(\vec{z}_T, \psi) * R(\vec{x}_T, \theta) * R(\vec{z}_S, \varphi)$$

Given a rotation matrix R, we can compute the Euler angles, ψ, θ, and φ by equating each element in R with the corresponding element in the matrix product $R_z(\psi)R_x(\theta)R_z(\varphi)$. This results in six equations that can be used to find the Euler angles.

Experimental results

A set of standard echography gestures with motion capture are performed on patients by experts. These medical gestures were analyzed to determine the orientation of the probe.

Figure 4 shows the Euler angles evolution. We chose to work on three organs: pancreas, portal vein and Gallbladder. The study was performed on fourteen patients and the curves presented are average measurements. A motion capture is performed over a period of 10 min with a frequency of 100 frames per second.

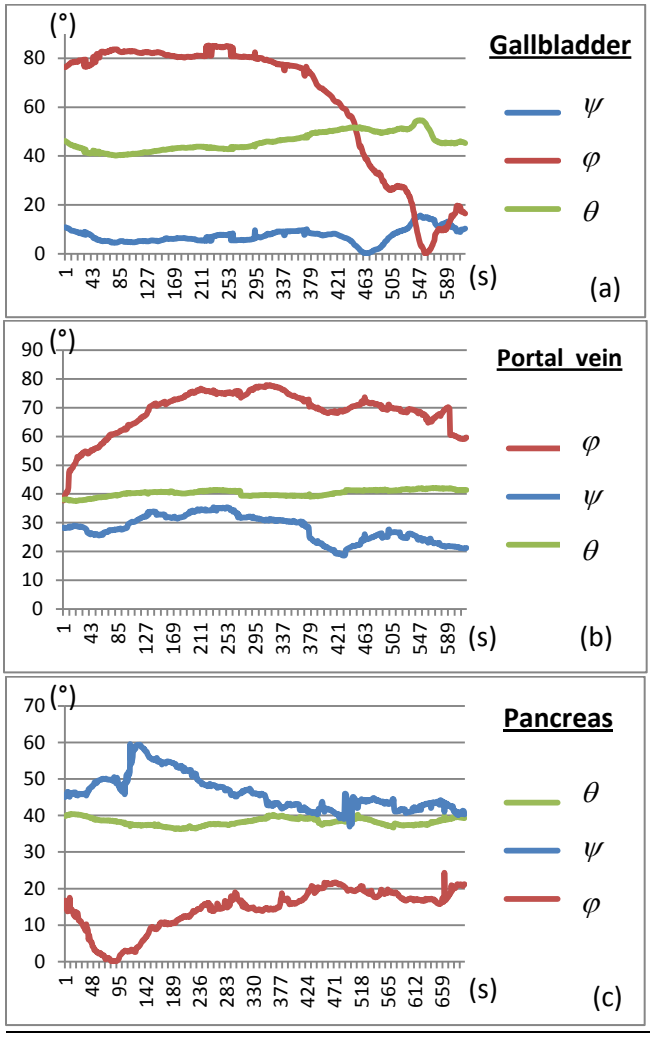

Figure 4 : Evolution of the Euler angles during a standard echography gesture, (a): Gallbladder, (b): Portal vein (c): Pancreas.

Through these curves, we can identify the maximum orientation of the probe. The values of Euler angles are presented in Table 1.

Table 1 : The maximum orientation of the probe during a standard echography act.

		Euler Angles		
		max : φ (°)	*max* : θ (°)	*max* : ψ (°)
Organs	Gallbladder	84.29	52.84	17.95
	Portal vein	77.34	41.46	34.63
	Pancreas	24.36	59.58	59.58

The obtained results will be used, in the next section, mainly in the definition of the kinematics specification and the description the workspace of the proposed manipulator.

KINEMATIC MODEL OF THE SLAVE ROBOT

In the last decade, tele-echography projects used serial architecture robots like TER [18], OTELO [19] or ESTELE [20]. Its principles have been patented. The robot architecture proposed in this paper is different from classical ones and from most robots used for tele-echography. The spherical parallel mechanism (SPM) has been selected because its characteristics meet the constraints requirements. This architecture offers an excellent stiffness, high precision and is light weight.

The SPM structure

The 3-RRR SPM device consists of two bodies, the base ① and the platform ②. ① and ② are connected by three RRR legs as shown in the joint graph of the Figure 5.

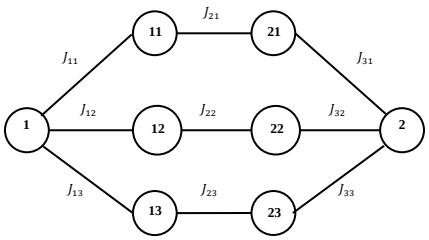

Figure 5 : The joint graph of the 3 RRR SPM

For each leg, the axes of the three revolute joints are intersecting in a single point *O* which is the center of the SPM (Figure 6).

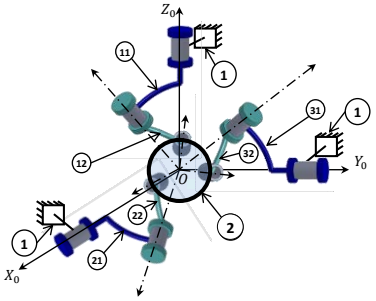

Figure 6 : Solid representation of the 3-RRR SPM

A solid representation of the 3-RRR manipulator is shown in Figure 6. The underlined R denotes the active revolute joint. The degree of freedom (dof) of the SPM is determined by means of the Chebychev-Kutzbach-Grübler formula [21], as given in equation (1). Here, we have the number of links n = 8 and the number of joints p = 9. The, the degree of freedom (*dof*) of this device is,

$$dof = 3(n-1) - 2p = 3(8-1) - 2 \times 9 = 3 \qquad (1)$$

So the platform ② has 3 dof spherical motions with respect to the base ①.

The three revolute joints with the base ① have orthogonal axes intersecting in the center O. This chosen configuration allows the platform ② to reach any point in the unit sphere of the three dimensional space. Xin-Jun Liu et al. [22] have shown that this geometric configuration of the base joint axes allows the platform to reach any orientation within the space defined by the joint limits.

Since, the SPM is the parallel association of three spherical serial robots then its workspace is reduced to the intersection of three workspace described by the three spherical serial robots.

A forward geometric model of a spherical serial robot allows us to identify the workspace of the SPM robot by means of the combination of three spherical serial robots as illustrated in Figure 6.

Notation and design parameters

Figure 7 shows a schematic of the SPM. The reference frame $\mathcal{R}_0(O, X_0, Y_0, Z_0)$ defines the fixed coordinate system and the reference frame defining the rotating platform is (O, X_p, Y_p, Z_p). The rotating platform is connected to the base through three legs, each of which comprises two arms and three revolute joints.

The design parameters under consideration are:

- the angles $\alpha_{i1}, i = 1,2,3$ which are for the angles between the three actuator axes and their corresponding revolute joints of outer arms
- the angles $\alpha_{i2}, i = 1,2,3$ which represent the angles between the two revolute joints of the legs
- Geometric parameters of the effector : $\beta_i, i = 1,2,3$ represent the angles measured between the $Z_p$axis of the platform frame and the center of the last revolute joint of the leg i.

These angles are also subject to the following geometrical constraints: $\alpha_{i1}+\alpha_{i2}+\beta_i<\pi/2, i=1,2,3$.

μ_1, μ_2, μ_3, in Figure 7-(b), represent the angles between (O, Z_p, Z_{3i}) and (O, Z_p, Z_{3i+1}) planes. The end-effector platform is assumed symmetrical, we consider that : $\mu_1 = \mu_2 = \mu_3 = \mu$

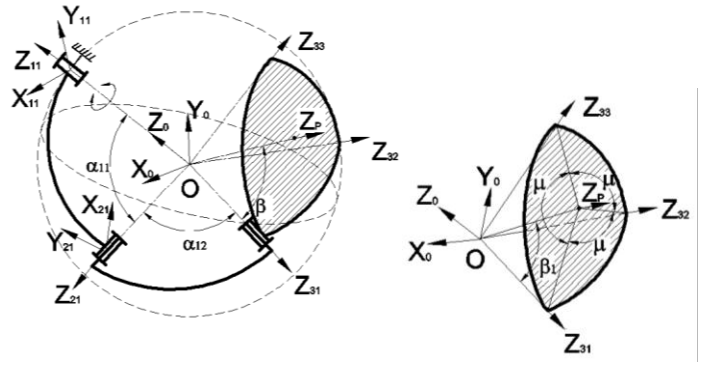

Figure 7 : Definition of design parameters: (a) a single leg RRR is represented, (b) a mobile platform

Kinematic model

The inverse kinematic model consists in finding θ_{1i}. for a given orientation of the mobile platform. This model can be obtained for each leg, RRR, thanks to the following relation:

$$Z_{3i} \cdot Z_{2i} = cos(\alpha_{i2}), i = 1,2,3 \quad (2)$$

Where the unknowns are the joint angles $\theta_{1i}, \theta_{2i}, \theta_{3i}$ (i=1,2,3) to be determined for a given location of the point P, the center of the mobile platform.

The terms of vectors Z_{2i} and Z_{3i} are expressed in the reference frame, $\mathcal{R}_0$, depending on the geometric parameters of the spherical manipulator, α_{i1}, α_{i2}, β_i and μ, and input variable θ_{1i}.

Expression of vector Z_{2i} in frame $\mathcal{R}_{2i}$

The vector Z_{2i} is obtained using the rotation matrix ${}^0R_{2i}$, from local frame $\mathcal{R}_{2i}$ to reference frame $\mathcal{R}_0$.

$$Z_{2i} = {}^0R_{2i} \cdot z_{2i} = [x_{Z_{2i}} \quad y_{Z_{2i}} \quad z_{Z_{2i}}]^T \quad (3)$$

Where,

${}^0R_{2i} = {}^0R_{1i}\,{}^{1i}R_{2i}$

For i=1 :

${}^0R_{21} = {}^0R_{11}\,{}^{11}R_{21} = I_{3\times3}R_Z(\theta_{11})R_X(\alpha_{11})$

For i =2 :

${}^0R_{22} = {}^0R_{12}\,{}^{12}R_{22} = R_X\left(\frac{\pi}{2}\right)R_Z\left(\frac{\pi}{2}\right)R_Z(\theta_{12})R_X(\alpha_{12})$

For i=3 :

${}^0R_{23} = {}^0R_{13}\,{}^{13}R_{23} = R_Y\left(\frac{\pi}{2}\right)R_Z\left(\frac{\pi}{2}\right)R_Z(\theta_{13})R_X(\alpha_{13})$

$z_{2i} = [0 \quad 0 \quad 1]^T$: The coordinates of the vector z_{2i} in the frame $\mathcal{R}_{2i}$.

Expression of vector Z_{3i} in frame $\mathcal{R}_0$

The vectors Z_{3i} is expressed in the reference frame using ZXZ Euler angles $[\varphi, \theta, \psi]$ as follows:

$$Z_{3i} = M_E z_{3i} = [x_{Z_{3i}} \quad y_{Z_{3i}} \quad z_{Z_{3i}}]^T \quad (4)$$

Where, M_E is the rotation Euler matrix (see Appendix A).

$z_{3i} = [x_{ip} \quad y_{ip} \quad z_{ip}]$ are the coordinates of the vector z_{3i}in the frame $\mathcal{R}_P$.

We note that the passive variables, θ_{2i} and θ_{3i}, do not appear in the final equation of inverse kinematic model.

Inverse kinematic model

The inverse problem is defined by equation (5), (i=1,2,3), for a given orientation of a platform $[\varphi, \theta, \psi]$.

$$\begin{bmatrix} x_{Z_{3i}} \\ y_{Z_{3i}} \\ z_{Z_{3i}} \end{bmatrix} \cdot \begin{bmatrix} x_{Z_{2i}} \\ y_{Z_{2i}} \\ z_{Z_{2i}} \end{bmatrix} - \cos\alpha_{2i} = 0 \quad (5)$$

In what follows, we detail the inverse kinematic model for leg i= 1.

For i=1, equation (5) is rewritten as:

$$Z_{31} \cdot Z_{21} - \cos\alpha_{21} = 0 \quad (6)$$

In the frame $\mathcal{R}_{31}$we have:

$$z_{31} = \begin{bmatrix} x_{Z_{31}} \\ y_{Z_{31}} \\ z_{Z_{31}} \end{bmatrix} = \begin{bmatrix} \sin\beta \\ 0 \\ \cos\beta \end{bmatrix} \quad (7)$$

The coordinates of vector Z_{31} in the reference frame $\mathcal{R}_0$are:

$$x_{Z_{31}} = \sin\beta\,(\cos\psi\cos\varphi - \sin\psi\sin\theta\sin\varphi) \quad (8)$$

$$y_{Z_{31}} = \sin\beta\,(\sin\psi\cos\varphi + \cos\psi\sin\theta\sin\varphi) + \cos\beta\,(-\cos\psi\sin\theta) \quad (9)$$

$$z_{Z_{31}} = \sin\beta\,(\sin\theta\sin\varphi) + \cos\beta\,(\cos\theta) \quad (10)$$

The coordinates of vector Z_{21} in the reference frame $\mathcal{R}_0$ are:

$$Z_{21} = \begin{bmatrix} x_{Z_{21}} \\ y_{Z_{21}} \\ z_{Z_{21}} \end{bmatrix} = \begin{bmatrix} \cos\alpha_{11} \\ \sin\alpha_{11}\sin\theta_{11} \\ -\sin\alpha_{11}\cos\theta_{11} \end{bmatrix} \quad (11)$$

Equation (5) has been derived for the first chain, i=1, and can be expressed as a function of $\cos(\theta_{11})$ and $\sin(\theta_{11})$ as follows:

$$x_{Z_{31}}\cos\alpha_{11} + y_{Z_{31}}\sin\alpha_{11}\sin\theta_{11} - z_{Z_{31}}\sin\alpha_{11}\cos\theta_{11} - \cos\alpha_{21} = 0 \quad (12)$$

This can be written as:

$$m_1\sin\theta_{11} + l_1\cos\theta_{11} - n_1 = 0 \quad (13)$$

Where,

$$\begin{cases} l_1 = -z_{Z_{31}}\sin\alpha_{11} \\ m_1 = y_{Z_{31}}\sin\alpha_{11} \\ n_1 = \cos\alpha_{21} - x_{Z_{31}}\cos\alpha_{11} \end{cases} \quad (14)$$

Or,

$$\begin{cases} l_1 = -(\sin\beta\,(\sin\theta\sin\varphi) + \cos\beta\cos\theta)\sin\alpha_{11} \\ m_1 = \left(\begin{matrix}\sin\beta\,(\sin\psi\cos\varphi + \cos\psi\sin\theta\sin\varphi) \\ +\cos\beta\,(-\cos\psi\sin\theta)\end{matrix}\right)\sin\alpha_{11} \\ n_1 = \cos\alpha_{21} - \left(\sin\beta\left(\begin{matrix}\cos\psi\cos\varphi \\ -\sin\psi\sin\theta\sin\varphi\end{matrix}\right)\right)\cos\alpha_{11} \end{cases} \quad (15)$$

Equation (13) can have a solution if and only if:

$$\left|\frac{n_1}{\sqrt{l_1^2+m_1^2}}\right| \leq 1 \Leftrightarrow n_1^2 - (l_1^2 + m_1^2) \leq 0 \quad (16)$$

In the general case, this equation becomes, for i=1,2,3:

$$S_i(\varphi,\theta,\psi) = n_i^2 - (l_i^2 + m_i^2) \leq 0 \quad (17)$$

The orientation workspace of the spherical parallel manipulator is defined as a region of the three-dimensional space that can be swept by a point on the platform. The only

constraints taken into account are the ones coming from the different legs given by equation (17), defined here by $S_i(\varphi, \theta, \psi)$.

OPTIMIZATION PROBLEM

Orientation workspace evaluation

After selecting the set of Euler angles for representing the mobile platform orientation, it remains to determine the way to represent the orientation workspace.

Three alternatives exist for representing the orientation workspace [23]. Here, we chose to represent the workspace in a cylindrical coordinate system, where Φ and Θ are the polar coordinates and Ψ is the z-coordinate. The representation of the orientation workspace is not the purpose of this work.

The design criterion of the SPM to maximize will be the size of the orientation workspace. To do this, we need to quantify the orientation workspace.

Ceccarelli et al. [24] proposed a method for calculating the volume of the workspace. We have adapted this method to our work to calculate "*the volume of the orientation workspace"*. We will consider this volume as the optimization criterion of the dimensions of the spherical parallel manipulator.

The volume of the robot is discretized in several elementary surfaces A_ψ, located in parallel planes. The sum of these elementary surfaces will be the volumeWA of the workspace.

$$WA = \sum_{\psi=\psi_{min}}^{\psi=\psi_{max}} \Delta\psi A_\psi \tag{18}$$

$\Delta\psi$ is the increment of the distance between two successive shots.

An elementary surface is calculated from the following expression :

$$A_\psi = \sum_{i=1}^{i_{max}} \sum_{j=1}^{j_{max}} \left(P_{ij} \Delta\varphi \Delta\theta\right) \tag{19}$$

Where, Δφ and Δθ are the elementary criteria of area located around a point assumed rectangular (see Figure 8)

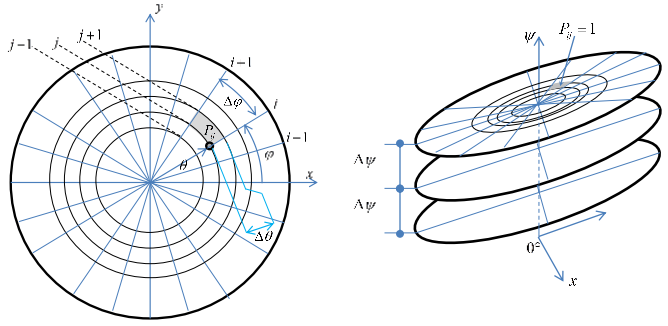

Figure 8 : A general scheme for binary representation and evaluation of manipulator orientation workspace**.**

The value of P_{ij} is given by:

$$P_{ij} = \begin{cases} 0 \text{ if } P_{ij} \notin \text{W} \\ 1 \text{ if } P_{ij} \in \text{W} \end{cases} \tag{20}$$

W indicates the workspace region.

Optimization problem

The optimization problem is formulated as follows: find the angles α_1 and α_2 of links orientation in each leg that maximize the volume of the orientation workspace.
That translates by Objective function:

$$Max\left(WA = \sum_{\psi=\psi_{min}}^{\psi=\psi_{max}} \Delta\psi A_\psi\right) \tag{21}$$

Subject to,

$S_i(\alpha_{i1}, \alpha_{i2}, \beta_i) \leq 0$

$\alpha_{i1} + \alpha_{i2} + \beta < \frac{\pi}{2}$

$(\alpha_{i1}, \alpha_{i2}, \beta_i) \in [0,2\pi], i = 1,2,3$

Application of the Genetic Algorithm

The genetic algorithm, GA, is a stochastic global search method that mimics the metaphor of natural biological evolution [14]. GA was selected as an optimization tool because it has benefits of both weak and strong search methods. Strong methods, such as numerical optimization procedures, perform a search in an informed manner by function gradients. Weak methods such as random or exhaustive procedures search in a uniformed method by extensively sampling the design space.

Weak methods are expensive but more likely to find optima; strong methods are inexpensive but more likely to settle by local sub optima.

GA operates with a strong progression toward improved designs, together with the weak operations of probabilistic selection, crossover and mutation. GA methods are robust because they simultaneously evaluate many points in the search space and more likely converge toward the global optimal solution.

In GA search, the goal is to find the maximal orientation workspace volume. Initially the algorithm generates 50 sets of different design parameters as the first generation parents. Next, the workspace volume with respect to each set of design parameters is calculated. Third the parents are ranked by their workspace volume. Each parent has a fitness number, which measures the size of its workspace. The parent with a large workspace volume is ranked as the best parent. Parents are selected according to their ranking to produce offsprings.

An elitist strategy is adapted. The most fit individual will probabilistically survive through successive generations. We use a generation gap, G_{gap}, and a fitness-based reinsertion to implement the elitist strategy where by the most fit individuals always propagate through to successive generations. Thus, (N_{ind}×G_{gap}) new individuals are produced at each generation. A reinsertion scheme must be used to determine which individuals are to exist in the new population.

Figure 9 shows the scheme of the genetic algorithm method applied to the design problem.

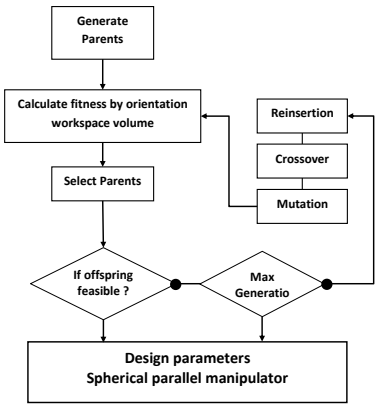

Figure 9 : Flow chart for GA method.

RESULTS AND DISCUSSION

Using a population size of 50, the genetic algorithm was run for 150 generations. A list of the best 50 individuals was continually maintained [21] during the execution of the genetic algorithm, allowing the final selection of solution to be made from the best structures found by the genetic algorithm overall generations.

Table 2 : The optimal parameters of spherical parallel mechanism

Design vector	
Workspace volume WA	253.8
α_{11}	45.2°
α_{12}	34.87°
α_{21}	45.1°
α_{22}	35.3°
α_{31}	44.89°
α_{32}	35°
β	9.22°
$0 \le \varphi \le 88.05$ / $0 \le \theta \le 89.05°$ / $0 \le \psi \le 88.9°$	

We performed a kinematic optimization in such a way as to maximize the workspace index WA. The new spherical parallel mechanism meets the orientation requirements identified during the motion capture (Table 1). The optimal parameters selected by the GA are presented in Table 2. A CAD model of the spherical parallel manipulator is developed in accordance with these specifications. Figure 10 represents the optimal design for the studied parallel mechanism. The final orientation workspace is given in Table 2.

A new prototype robot will be designed and manufactured on the frame of this mechanical architecture. Then it will be used by medical doctors and its performances compared with ones of the serial architectures.

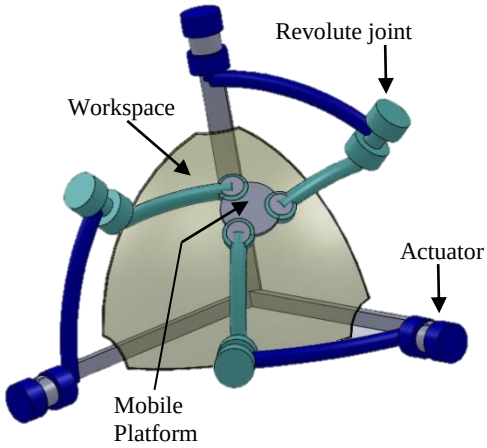

Figure 10: An optimal spherical parallel mechanism.

ACKNOWLEDGMENTS

This research is supported by the CPER Poitou-Charentes 2007-2013 (program project 10 'Images et inter-activites').

REFERENCES

1 G. Kontaxakis, S. Walter, and G. Sakas. Eu-teleinvivo: An integrated portable telemedicine workstation featuring acquisition, processing and transmission over low-bandwith lites of 3-D ultrasound volume image. *Proc. Information Technology Applications in Biomedicine (ITAB)* (2000), 158–163.

2 F. Pierrot, E. Dombre, E. Dégoulange, L. Urbain, P. Caron, S. Boudet, J. Gariépy, and J.Mégnien. Hippocrate: A safe robot arm for medical applications with force feedback. *Med. Image Anal.*, 3 (1999), 285–300.

3 P. Abolmaesumi, S. E. Salcudean, W.-H. Zhu, M. Sirouspour, and S. DiMaio. Image-guided control of a robot formedical ultrasound. *IEEE Trans. Robot. Automat.*, , vol. 18 (Feb. 2002), 11–23.

4 D. D. Cunha, P. Gravez, C. Leroy, E. Maillard, J. Jouan, P. Varley, M. Jones,M. Halliwell, D. Hawkes, P.Wells, and L. Angelini. Themidstep system for ultrasound guided remote telesurgery. *Proc. 20th Annu. Int. Conf. IEEE Engineering in Medicine and Biology Society* (1998), 1266–1269.

5 M. Mitsuishi, S. Warisawa, T. Tsuda, T. Higuchi, N. Koizumi, H. Hashizume, and K. Fujiwara. Remote ultrasound diagnostic system. *Proc. IEEE Int. Conf. Robotics and Automation* (2001), 1567–1574.

6 P. Abolmaesumi, W.-H. Zhu, S. DiMaio, and M. Sirouspour. A user interface for robot-assisted diagnostic ultrasound. *IEEE Int. Conf. Robotics and Automation (ICRA)* (2001), 1549–1554.

7 A. Gourdon, P. Poignet, G. Poisson, Y. Parmantier, and P. March. Master–slave robotic system for ultrasound scanning. *Proc. Eur. Medical and Biological Engineering Conf.*, vol. II (Mar. 1999), 1116–1117.

8 K. Masuda, E. Kimura, N. Tateishi, and K. Ishihara. Three-dimensional motion mechanism of ultrasound probe and its application for tele-echography system. *Proc. IEEE/RSJ Int. Conf. Intelligent Robots and Systems* (2001), 1112–1116.

9 Z. Affi, L. Romdhane, A.Maalej. Dimensional synthesis of a 3-translational-dof in-parallel manipulator for a desired workspace. *Eur. J. Mech. A/Solids* , 23 (2) (2004), pp 311–324.

10 M.A. Laribi, L. Romdhane, S. Zeghloul. Analysis and dimensional synthesis of the DELTA robot for a prescribed workspace. *Mech. Mach. Theory 42 (7)* (2007), pp) 859–870.

11 A. Kosinska, M. Galicki, K. Kedzior. Designing and optimization of parameters of Delta-4 parallel manipulator for a given workspace. *J. Rob. Syst. 20 (9)* (2003), pp 539–548.

12 Romdhane, L. Orientation Workspace of Parallel Manipulators. *The European Journal of Mechanics/A Solids.* , Vol. 13, No. 4, (1994).

13 Gregorio, R. Di. Kinematics of a new spherical parallel manipulator with three equal legs: the 3-URC wrist. *J. Rob. Syst. 18 (5)* (2001), pp. 213–219.

14 GREGORIO, R. Di. The 3-RRS Wirst : A new, simple and non-overconstrained spherical parallel manipulator. *Journal of Mechanical Design*, Vol 126 (2004), pp 850-855.

15 Bai, Shaoping. Optimum design of spherical parallel manipulators for a prescribed workspace. *Mechanism and Machine Theory*, Volume 45, Issue 2 (February 2010), 200-211.

16 Cavanagh, G. Wu and P.R. ISB recommendations for standardization in the reporting of kinematic data. *Journal of Biomechanics*, Volume 28, Issue 10 (October 1995), 1257-1261.

17 Gleicher, M. Retargetting motion to new characters. *Proceedings of the ACM SIGGRAPH Conference on Computer Graphics* (1998), 33–42.

18 Adriana Vilchis, Jocelyne Troccaz, Philippe Cinquin, Kohji Masuda and Franck Pellissier. A New Robot Architecture for Tele-Echography. *IEEE TRANSACTIONS ON ROBOTICS AND AUTOMATION*, 19, 5 (OCTOBER 2003).

19 F. Courreges, P. Vieyres and R.S.H. Istepanian. Advances in robotic tele-echography services - the OTELO system. *IEEE Int. Conf. Engineering in Medicine and Biology Society*, II (Sept 2004), 5371 - 5374.

20 L. Nouaille, N. Smith-Guérin, G. Poisson and P. Arbeille. Optimization of a 4 dof tele-echography robot. *IEEE/RSJ International Conference on Intelligent Robots and Systems* (October 2010), 3501-3506.

21 Angeles, J. *Ralionalli'inCllwtics*. Springer-Verlag, New York, 1988.

22 Xin-Jun Liu, Zhen-Lin Jin and Feng Gao. Optimum design of 3-DOF spherical parallel Manipulators with respect to the conditioning and stiffness indices. *Mechanism and Machine Theory*, 35 (2000), 1257-1267.

23 Ryu, Ilian A. Bonev and Jeha. ORIENTATION WORKSPACE ANALYSIS OF 6-DOF PARALLEL MANIPULATORS. In *Proceedings of the ASME Design Engineering Technical Conferences* (Las Vegas, Nevada September 12-15, 1999,).

24 M. Ceccarelli, G. Carbone, E. Ottaviano. An Optimization Problem Approach For Designing Both Serial And Parallel Manipulators. *The Int. Sym. on Multibody Systems and Mechatronics Uberlandia, Brazil, 6-9 March* (2005).

25 H., HOLLAND J. *Adoptation in Natural and Artificial Systems*. The University of Michigan, 1992.

26 A. Kosinska, M. Galicki, K. Kedzior. Designing and optimization of parameters of Delta-4 parallel manipulator for a given workspace. *J. Rob. Syst.*, 20, 9 (2003), 539–548.

ANNEX A

THE ROTATION EULER MATRIX

$$M_E = \begin{bmatrix} \cos\psi\cos\varphi - \sin\psi\sin\theta\sin\varphi & -\cos\psi\sin\varphi - \sin\psi\cos\theta\cos\varphi & \sin\psi\sin\theta \\ \sin\psi\cos\varphi + \cos\psi\cos\theta\sin\varphi & -\sin\psi\sin\varphi + \cos\psi\cos\theta\cos\varphi & -\cos\psi\sin\theta \\ \sin\theta\sin\varphi & \sin\theta\cos\varphi & \cos\theta \end{bmatrix}$$